UNIVERSITY OF CALIFORNIA,
IRVINE

Improving Assay Performance using Microfluidic Cavity Acoustic Transducers

THESIS

submitted in partial satisfaction of the requirements
for the degree of

MASTER OF SCIENCE

in Biomedical Engineering

by

Imaly Anoshka Nanayakkara

Thesis Committee:
Professor Abraham Lee, Chair
Professor William Tang
Assistant Professor Elliot Hui

2014

TABLE OF CONTENTS

LIST OF FIGURES

LIST OF TABLES

ACKNOWLEDGMENTS

First and foremost, I would like to express my deepest gratitude to Professor Abraham P. Lee, my committee chair and advisor. Your guidance and support has shaped me into becoming a better researcher and I'm truly grateful for the experience and opportunity.

I would like to thank my committee members, Professors William Tang and Elliot Hui, for being kind enough to review my thesis and offer feedback.

I would like to thank Rie Nakajima and Al Jasinskas from the Felgner lab for always encouraging me and providing support when my immunoassays went awry. Your excitement for this project was infectious and motivated me to keep persevering. I'm so grateful for having the opportunity of working with you both.

I would like to thank all the members of the BioMiNT lab. Your camaraderie and friendship have made the past two years so memorable. I would like to thank Dr. Maulik Patel and Dr. Mindy Simon for being such a wonderful mentors to me, for both science and life. I've learned so much from you and am thankful for your encouragement, support and friendship. I'll never forget our silly conversations and all the great times we've had. I would like to thank Crystal Rapier; despite having a short friendship, we've shared so many memories that I won't forget. I'd like to thank Apurva Patel for all his help with microfabrication as well as Steven, Derek and Willy for all the laughter and joy you four brought to lab. I would like to thank the rest of the BioMiNT lab for being wonderful colleagues.

Lastly I would like to thank my family, especially my parents and brother, who always push me to be better. I'm so blessed to have such support and love.

ABSTRACT OF THE THESIS

Improving Assay Performance using Microfluidic Cavity Acoustic Transducers

By

Imaly Nanayakkara

Master of Science in Biomedical Engineering

University of California, Irvine, 2014

Professor Abraham P. Lee, Chair

The development of an integrated immunoassay platform is crucial for providing diagnostic tools for global health applications. With the emergence of microfluidics, there is an increased focus in addressing this need. While many platforms have been created to successfully complete an immunoassay, they still require bulky external equipment to manipulate fluid within the device. Using technology developed in the BioMiNT lab, we've created an immunoassay platform that is capable of on-chip pumping and mixing with lateral and vertical-cavity acoustic transducer (LCAT & VCAT respectively) coupled to a piezoelectric transducer (PZT). PDMS devices were fabricated, molded and bonded to glass slides adhered with antigen-spotted nitrocellulose pads. Once they are primed with blocking buffer to introduce air bubbles, the devices are actuated with a PZT to drive fluid pumping and mixing. The reagents are pumped into the device serially and after completion, the spotted antigens on the pad become a dark purple hue, indicating an antibody-antigen binding event. For quantitative results, the intensities are evaluated using computer software. Results show that the resulting spot intensities are comparable to an established, optimized microarray platform in one-fifth of the time. We also show that these results cannot be reproduced in a passive or flow-through microfluidic device, indicating that convective mixing is necessary for improved signal intensity. Using the LCAT/VCAT platform, an immunoassay can be performed in 20 minutes and with increased sensitivity. Future work will involve expanding the device to allow for an automated point-of-care platform.

Chapter 1
Introduction

1.1 Problem Statement

Currently, 80% of all deaths caused by infectious diseases occur in developing nations, claiming 12 million lives per year [1]. However, this statistic falls to less than 5% in developed nations, where these diseases are routinely tested and treated [2]. The drastic difference is due the lack of access to healthcare in underdeveloped nations. The absence of healthcare facilities stems from insufficient infrastructure and the lack of clean water and electricity to support laboratories that are common in developed nations [3]. Additionally, there is a shortage of trained personnel to perform tests and analysis; coupled with the high cost of diagnostics, it becomes increasingly difficult to provide traditional means of disease control and treatment. As a result, there is an urgent need for the development of a cost-effective platform for diagnosing diseases in developing countries. With the development of point-of-care (POC) devices using microfluidics, novel devices are being actualized to combat the issues mentioned above and provide critical information needed for disease diagnosis.

1.2 Proposed Solution

The first step in prevention and treatment of any disease is accurate and timely diagnosis [3]. However, the current prevalent methods in developed nations cannot be translated for use in resource-limited settings, as they require "state-of-the-art" facilities and medical professionals. The lack of infrastructure and electricity cannot support the instrumentation required to carry out sample preparation, purification, testing and analysis of a given patient sample [3]. Therefore, a system must be designed that will effectively integrate several of the aforementioned steps to move towards sample-to-answer devices. Existence of such technology will allow for greater access to healthcare worldwide.

Current methods for diagnosing infectious diseases are enzyme-linked immunosorbent assays (ELISA) and polymerase chain reaction (PCR). Both of these processes test for the presence of specific biomarkers of the given disease and require bulky and expensive instrumentation for testing and detection. Each process requires a standard kit, which contains all the necessary reagents and is also high in cost. Additionally they require technicians who are trained to perform these tests and to use and troubleshoot the necessary machinery. Given the rural environments of most underdeveloped nations, they cannot support these types of instrumentation and therefore, cannot use these traditional means. Because of these obstacles, there has been increased focus in developing lab-on-a-chip (LOC) devices, which are capable of translating these processes from bench to bedside.

The field of microfluidics presents many advantages when fabricating a micro total analysis system (uTAS) for POC use. Because these systems require low sample and reagent volumes and a smaller footprint, it is ideal for use in resource-limited areas. Many platforms have been developed that translate the ELISA and PCR processes to a microfluidic device however they still rely heavily on cumbersome external pumps to deliver fluids. These pumps require a stable power source which may not be available in all testing environments so novel technologies are being actualized that maintain the small size and minimal complexity of microfluidic devices and are portable for POC use. The Lateral Cavity Acoustic Transducer (LCAT) developed by Dr. Abraham Lee's Biomolecular Microsystems and Nanotranducers Lab aims to accomplish this with the use of cavity-induced microstreaming actuated by a piezoelectric transducer. This microstreaming arises from side channels that trap air to form an air-liquid interface. When the device is coupled with a piezoelectric transducer, the interfaces oscillate and can pump and mix fluid depending on the orientation of the cavity. With this technology, on-chip mixing and pumping have been demonstrated and therefore, facilitate a portable, low-powered platform.

Another drawback of both ELISA and PCR is that they only test for the presence or absence of a particular protein. While this is the most straightforward method of diagnosing a disease, it can also be misleading as the presence of a one expression of protein can point

to a number of developing ailments. However, with biomarker discovery and the rising field of proteomics, we can only better understand the progression of a disease for any given patient but appropriately diagnose the disease for its given stage of infection. Dr. Phil Felgner's Protein Microarray Laboratory has focused on developing a microarray with different key biomarkers for several different diseases and because of their increased sensitivity and specificity, these arrays can be developed for diagnostic uses.

To create a novel POC device, the LCAT and protein microarray technologies were combined to allow for separate delivery of each of the reagents used in a given assay. By having individual LCAT pumps for each reagent, the automated platform facilitates ease of use and training. The LCAT also provides microstreaming that allows for enhanced mixing of reagents to decrease binding times so that the run time of each device is less compared to a traditional immunoassay. By exploiting the characteristics of acoustic transducers, a platform capable of on-chip pumping and mixing is rendered to address current healthcare obstacles.

1.3 Scope of Report

This report recounts the motivation, design, and results of a microfluidic immunoassay platform capable of on-chip pumping and mixing that is targeted for use in resource-limited settings. There is a holistic review of current similar technologies, detailing their strengths and shortcomings. The experimental design and testing process is overviewed, as well as key findings that led to the characteristics of the current system. The development of an electronics component is reviewed to show that this platform can be automated to better facilitate a POC device. This text concludes with a summary of the overall project and discussion of recommendations for future work.

1.4 Summary of Conclusions

At the conclusion of this project, a platform has been designed that is capable of pumping and convective mixing for immunoassay platforms. Results using the microfluidic platform have shown comparable spot intensities to that of an established optimized microarray platform. The sensitivity of the immunoassay has improved with the microfluidic design with the use of a lower dilution of secondary antibody solution. Comparisons to devices where reagents were sitting passively in the device and reagents that were only pumped and not mixed in the device show that localized acoustic cavity-induced convective mixing is essential to an improved signal. The use of an immunoglobulin-G (IgG) assay shows preliminary findings that an acoustic-driven microfluidic device can successfully complete an immunoassay with the use of piezoelectric transducer. Future work will involve expanding both the device and immunoassay so that reagents for an immunoassay using human serum can be introduced independently with the use of separately actuated PZTs. The findings presented in this report show promise for its potential use for point-of-care applications.

Chapter 2
Background

2.1 Current diagnostics

Most of the infectious diseases that are responsible for deaths worldwide are viral and bacterial diseases. Consequently, diagnosing these diseases requires detecting either RNA or DNA transfected from the viral host or detecting the characteristic antibodies associated with each disease. Traditional means involve running PCR and ELISA, respectively. PCR is a nucleic acid test that involves separating a sample of double stranded DNA and replicating a short segment using a specific primer that anneals to a target sequence of DNA [4]. If the target sequence is present in the DNA, the DNA will be replicated exponentially depending on the number of thermal cycles. The segments can then be detected using a probe, such as SYBR Green, which binds to double-stranded DNA and produces a color signal. Additional equipment is required to quantify the amount of signal produced.

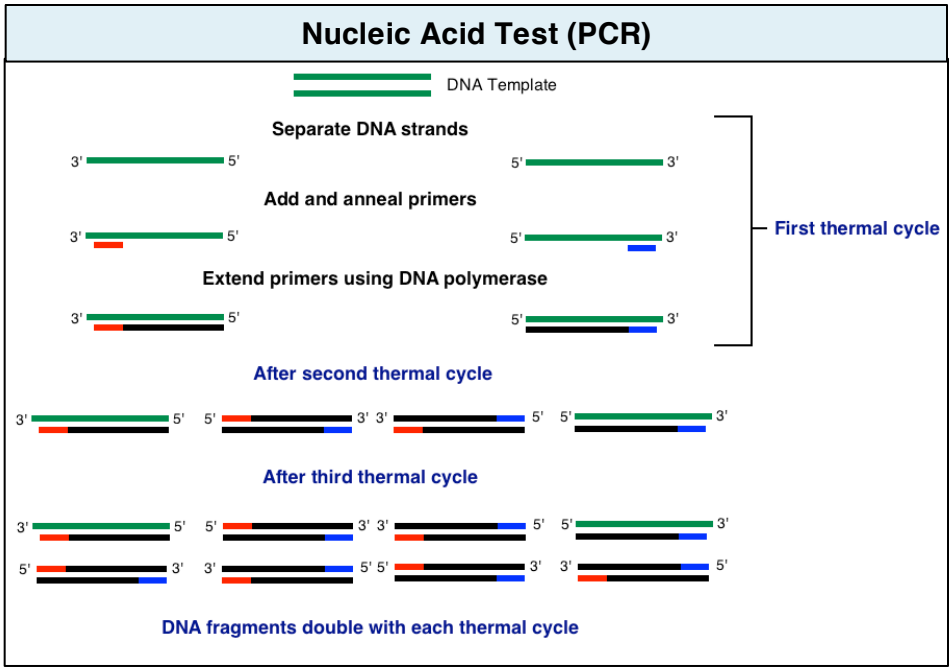

Figure 1. Illustration of PCR. Green lines represent the original DNA template. Red and blue lines represent primers for each strand and black lines represent the extension of these primers using DNA polymerase.

ELISA is an antibody test that involves testing for the antigens or antibodies produced by the viral DNA by using secondary antibodies to bind to the sample to detect the presence of the bound complexes [5]. A substrate solution is used during the final steps to produce a color signal and the subsequent intensity quantification is correlated to protein concentration. Again, additional equipment is required for signal measurement.

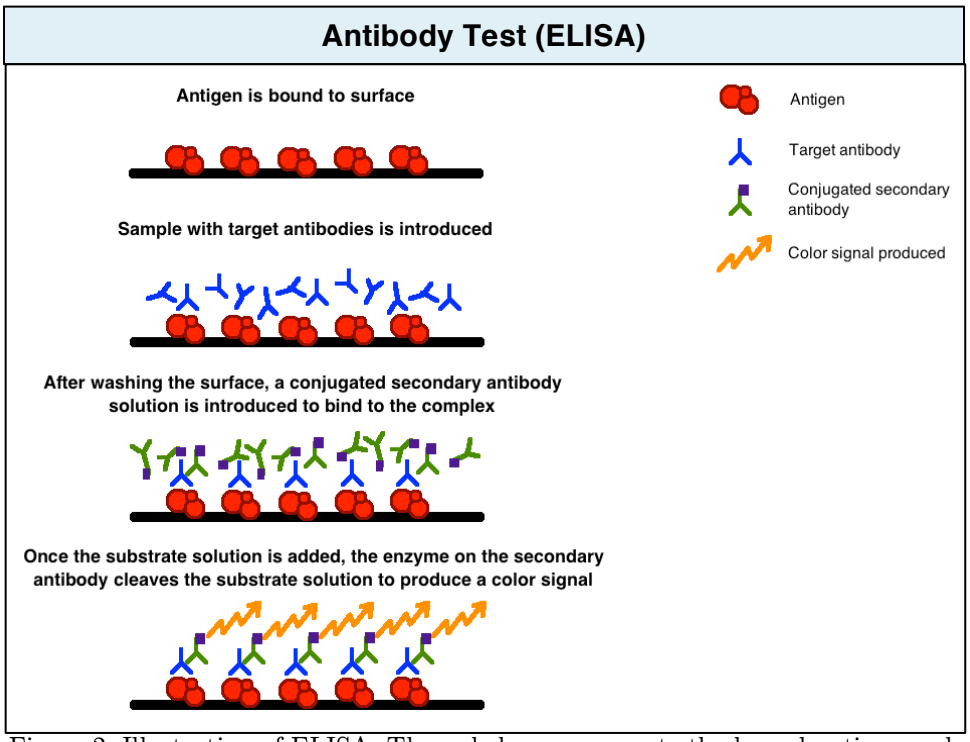

Figure 2. Illustration of ELISA. The red shape represents the bound antigen and the blue structure represents the target antibody present in a patient sample. The green structure with the purple addition represents the secondary antibody conjugated to an enzyme and the orange structure represents the color signal emitted when the enzyme is cleaved in the presence of a substrate solution.

Both processes rely on a centralized laboratory setting, as they require sterilized environments with access to clean water and electricity. In addition both these processes are time consuming and involve expensive reagents, kits and equipment. In developing nations, there are few laboratories with the necessary facilities, personnel and other required resources for successful functionality and maintenance. With these disadvantages in mind, there is a collective effort in the scientific community to create a POC device that addresses

these design constraints without compromising the sensitivity and specificity of these methods.

One of the few current diagnostic technologies that is well-suited to resource-limited settings are lateral flow tests, or immunochromatographic strip tests (ICS). These simple devices rapidly detect the presence or absence of a specific analyte. A common example of a lateral flow test is an at-home pregnancy test, however ICS tests have been developed for diagnosing several sexually-transmitted infections as well as infectious diseases such as HIV and hepatitis B [6, 7]. ICS tests usually have five main regions: a sample pad, a conjugate-pad, the test line, the control line and an absorbent pad. The sample pad is where the patient sample is applied and the sample is wicked downstream to react with the conjugate pad. The conjugate pad houses antibodies specific to the target analyte in the sample that are conjugated to a probe for detection (usually gold particles or dyed microspheres). As the reacted sample continues downstream, it will pass both the test line and the control line. From the conjugate pad to the absorbent pad lies a membrane, normally made of nitrocellulose. This membrane houses both the test line and the control line and is responsible for the one-directional fluid flow observed in the diagnostic, as well as protein-binding capacity and capillary flow rate. These characteristics stem from the membrane's porosity, pore size and polymer composition [8]. The test line houses anti-target analyte antibodies, immobilized to the surface, so that if the sample contains the analyte, it will bind to this surface. On the control line, antibodies specific to the detection probe are immobilized to the surface that will bind to the probes that were stored in the conjugate pad. Regardless of whether there is analyte in the sample, the control line will indicate proper functioning of the device. Lastly the remaining fluid will continue to the absorbent pad that acts as a waste reservoir.

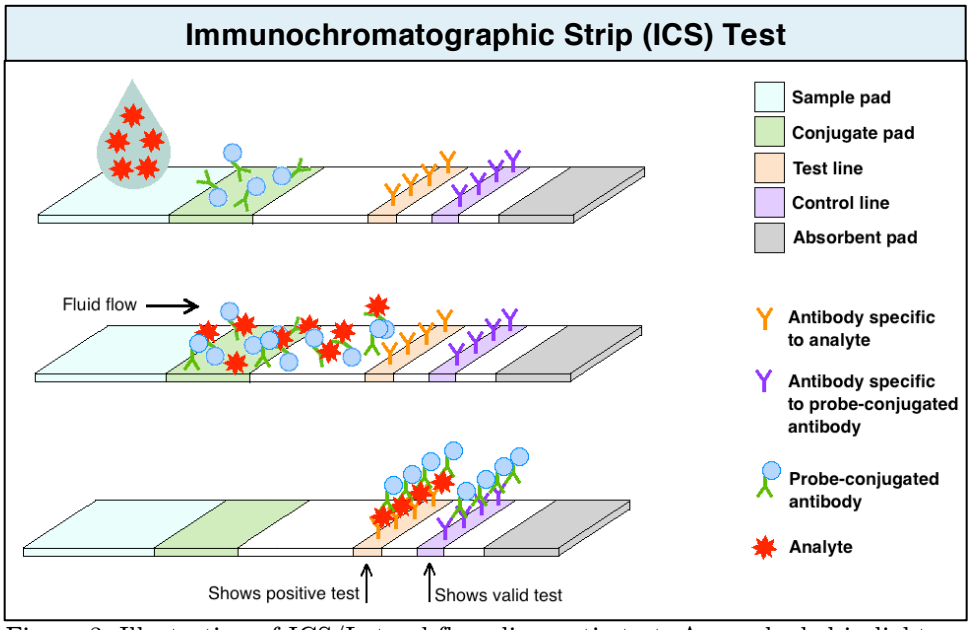

Figure 3. Illustration of ICS/Lateral flow diagnostic test. Areas shaded in light blue, light green, orange, light purple and gray represent the sample pad, conjugate pad, test line, control line and absorbent pad respectively. Structures in orange are antibodies specific to the analyte, structures in purple are antibodies specific to the antibody-probe and the green structures represent the antibody conjugated to the probe. Red shapes represent the analyte.

ICS tests allow for rapid POC diagnosis in areas with poor infrastructure to support equipment and facilities for traditional means. They are also well suited for these areas as they don't require refrigeration, are relatively inexpensive and are easy to use. Most importantly, the sensitivity of ICS tests are comparable to standard laboratory methods [9]. However, there are several drawbacks. These tests are normally qualitative in nature, limiting the diagnosis to binary response of analyte being present. Additionally, many of these tests are limited to the detection of one analyte, which may not provide enough information on the disease's progression [10]. However, despite these drawbacks, ICS tests are one of the very few diagnostic tools that have been successfully implemented in the developing world.

2.2 Theory and Introduction of Microfluidics

Passive immunoassay platforms rely heavily on external shakers and long incubation times to complete binding reactions due to these reactions being driven by diffusion at the macroscale. Diffusion-driven reactions can be represented by Fick's law, as shown below [11]:

$$\frac{\partial C}{\partial t} = D\nabla^2 C - \vec{u}\nabla C \qquad (1)$$

C represents the concentration of the analyte in bulk phase, D is the diffusivity of the analyte and u is the bulk velocity of the fluid. According to equation 1, the binding reaction, or the change in analyte concentration, depends heavily on the diffusivity and fluid velocity. At the microfluidic length scale, laminar flow is more readily observed than turbulent flow and as a result, transport is diffusion-based. However, by incorporating specific design features within a microfluidic device, convective transport can be introduced to drive mixing processes.

The field of microfluidics can help bridge the gap of providing health care to the most remote of regions since these platforms address the design constraints observed in the developing world and have innate advantages in their length scale, elaborated below. When Manz et al. first realized the possibility of creating an LOC device using the small characteristics of microchips, the development of a miniaturized total analysis system (uTAS) became the focus of many research groups. At these smaller length scales, there is increased fluid control due to well-defined laminar flow, controllable diffusion and surface forces dominating over gravitational forces [12]. Additionally there are the obvious characteristics in that a uTAS are portable and small in nature and require less sample volume therefore decreasing the footprint of diagnostic devices. For assays, there is improved performance as a result of higher sensitivity and a shorter sample-to-answer time.

The Peclet number is a non-numerical dimension used to determine whether transport is driven by convection or diffusion, shown below:

$$Pe = \frac{V_m H}{D} \qquad (2)$$

Vm represents the average velocity within the channel, H represents the channel height and D is the diffusivity of the biomolecule. When the Peclet number is greater than 1, transport is driven by convection and when it is less than 1, transport is driven by diffusion. By increasing the velocity and optimizing the height of the channel, convection can be easily introduced into a microfluidic platform to allow for fast binding times and improved performance of an immunoassay.

2.3 Current microfluidic platforms

Using the advantages that microfluidics presents, a LOC or uTAS device would be a well-suited solution for providing diagnostic tools for resource-limited settings. As a result, many research groups have focused on developing devices to translate macroscale processes to a miniaturized platform. Examples of such processes include separation and sorting [13-15]. By expanding these separate modules, they can be integrated so that PCR and ELISA can be implemented in a microfluidic device. Below are two examples of LOC platforms geared towards PCR applications.

Marcus et al. have developed an integrated device capable of cell capture and lysis, mRNA purification, cDNA synthesis and cDNA purification for real time-PCR applications. The design involves taking advantage of the elastic properties of polydimethylsiloxane (PDMS) by using a series of valves, controlled by pressure sources that will remain stagnant or expand over a fluidic channel to allow or block flow. These pressure sources can be actuated an off-chip Labview program. On the device there are separate nodules for each process for isolation, synthesis and purification. The fully integrative device is capable of attaining samples an order of magnitude larger than traditional means and detecting a large range of sample concentrations, spanning four orders of magnitude [16]. Despite the disadvantages of having bulky external pressure sources to drive the device and the complications of mass-production of such devices, the effort demonstrates having multiple parallel reactions in one platform.

By taking advantage of capillary electrophoresis, Liu et al. have created an integrated device that performs PCR amplification and DNA microarray detection from sample-to-answer analysis. The platform contains three components: a plastic chip, a printed-circuit board (PCB) and a Motorola eSensor microarray chip. The plastic chip houses the sample preparation, PCR chamber and the DNA microarray, as well as valves and piezoelectric transducers (PZT) for fluid flow and mixing. The PCB supplies the resistive heaters necessary for PCR and controls the chip's valves and mixing capability. Lastly, the Motorola eSensor detects electrochemical signals resulting from the DNA binding to immobilized nucleotides on the eSensor surface. With this device, Liu et. al were able to show low-abundance and high-abundance DNA detections [17]. The group takes into consideration the ease of fabrication by creating components that are simple and inexpensive as well as manufacturing concerns by machining the chip on polycarbonate and integrating the circuitry using a PCB and eSensor. While the technology relies on external ac volammetry to gather the signals detected, it provides a point-of-care approach to PCR while addressing concerns of manufacturing, sample volumes and sensitivity.

2.3.1. Microfluidic immunoassay platforms

Since many diseases are characterized by the presence or absence of distinct antibodies, immunoassays allow for quantification of these antibodies by correlating the amount of signal to a concentration and consequently, determining the progression of a disease. Examples of diseases that are currently diagnosed with immunoassays are HIV, tuberculosis, West Nile, etc.[18-20]. With infectious diseases being so prevalent in resource-limited areas, establishing a low-cost, low-power microfluidic platform would greatly improve a region's access to healthcare. Below are two examples of platforms that have been developed with this goal in mind.

A popular platform developed especially for resource-limited settings is the mChip from the Sia lab at Columbia University. Using plastic as the cartridge material, the device houses

two modules: storage and assay. In the storage module, the reagents are serially introduced through the device using air spacers to separate each one; this includes all the antibody solutions as well as wash and substrate solutions [18]. In the assay module, there are four detection areas that serve as a negative control, a test area and two positive controls to confirm the viability of the two different antibodies involved [21]. A silver film develops in the presence of a binding event, and by measuring the intensity of the silver film, the concentration of human HIV antibody can be determined. Their recent work has involved expanding the chip so that the results are analyzed with a customary reader that is easy to use; key features include the use of minimal patient sample (less than 1ul of whole blood), low power with 9V battery source, a communications nodule to send data to satellite servers and automation of reagent delivery with the use of a diaphragm micropump [21]. The mChip addresses the design issues mentioned earlier and is currently going through clinical trials. However, the reader components alone cost about $1000 [21]. By simplifying the device design and the driving mechanisms necessary to flow fluid through the device, the costs can be reduced so that it can become better amenable to these environments.

Bhattacharyya et. al developed a platform to test for C-reactive protein, an indicator for inflammation or infection which has been currently used to evaluate a patient's risk for cardiovascular disease [22]. A robust device was fabricated by hot embossing cyclic polyolefin to a silicon mold. Human serum containing CRP antigen is first flowed through the device, followed by two antibody solutions and a substrate solution to start a chemiluminescent reaction. To detect the reaction, an X-ray film is placed above the device so that the emitted light exposes the film. When evaluating the performance of the assay, the microfluidic assay produced higher signal than an immunoassay performed in a 96-well plate, therefore providing a viable replacement of traditional methods [23]. This device was fabricated as a proof-of-principle experiment and has not been further developed. However, this platform still provides a diagnostic solution to developing regions as it requires minimal set-up time, performs the assay in under 30mins, detects CRP concentrations at medically-relevant ranges and by using hot-embossing manufacturing, reduces production costs without compromising the robustness of the platform[23].

2.4 Acoustic microstreaming and Cavity Acoustic Transducers

Acoustic microstreaming is a phenomenon where fluid manipulation occurs because of energy being dissipated from a bubble's oscillating interface. This oscillating interface is observed when the bubble is coupled with an acoustic energy source, such as a piezoelectric transducer (PZT). This behavior was first observed by Elder and Nyborg and laid the foundation for explaining how microstreaming patterns are affected by amplitude and liquid viscosity [24]. However, because the fluid could only be manipulated near the boundary of the oscillating surface, microstreaming applications were limited until the development of microfluidic technologies emerged [25].

Because of the length scale and the micrometer resolution achieved with the microfabrication process, cavities can be specifically designed within the features of a device so that air bubbles can be strategically trapped to better exploit the observed microstreaming. Depending on the orientation of these bubbles in relation to the features in a device, the microstreaming generated can be employed to carry out different processes. Examples of such processes include cell lysing [26], DNA hybridization [27], fluid pumping and mixing [28, 29] and cell sorting [30].

There are two characteristic flows that are observed with acoustic microstreaming. The oscillating flow field is observed as the vibrations on the air-liquid interface of the bubble. The magnitude of this flow can be represented by the following equation:

$$U_o \sim d \cdot \omega \qquad (3)$$

where U_o is the velocity of the oscillating flow, d is the oscillation amplitude and ω is the angular frequency of the acoustic field. A secondary flow field is observed, which stems from the net displacement of the fluid, in response to U_o [25]. This secondary flow is known as the streaming flow and can be represented by the following equation:

$$U_s \sim \frac{{U_O}^2}{\omega \cdot R} \qquad (4)$$

where Us is the velocity of the streaming flow, Uo is the velocity of the oscillatory flow, ω is the angular frequency mentioned above and R is the length scale of the interface.

To take advantage of these two velocities, air bubbles must be strategically placed within the device so that fluid can be either mixed or pumped. Liu et al. first demonstrated mixing using cavity acoustic transducers for vesicle deformation, where the device trapped air bubble above a channel and when actuated, introduced localized streaming [29]. For the purposes of this manuscript, cavities placed above a feature are known as vertical-cavity acoustic transducers (VCAT). Our lab has previously shown how VCATs can be optimized both for mixing and hybridization purposes [27].

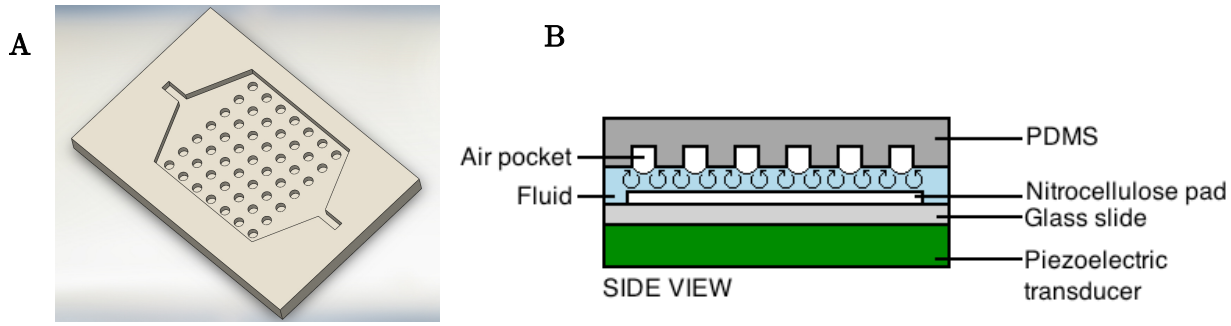

Figure 4. VCAT Illustrations. (A) Bottom-to-top rendering of a chamber with VCATs at the top. (B) Side view of VCATs actuated by a PZT. Beneath the air pockets, vortices indicating the microstreaming patterns observed lie adjacent to the interface.

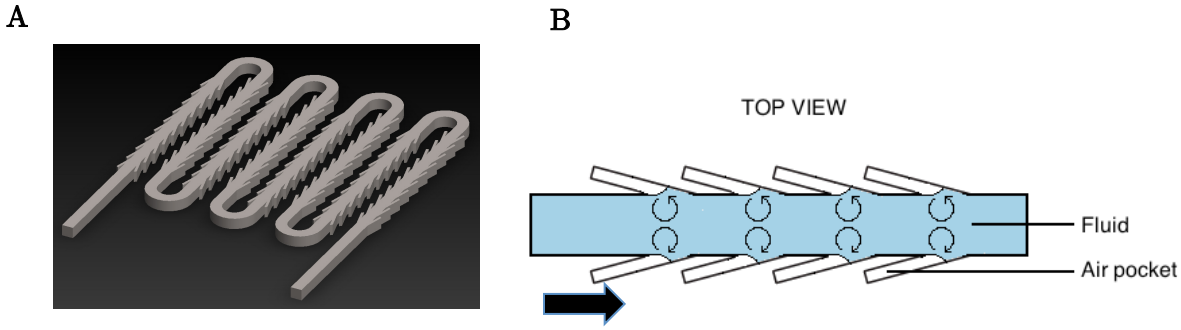

Figure 5. LCAT Illustrations. (A) Top-view rendering of an LCAT array. (B) Top view of LCATS actuated by a PZT (not illustrated). The microvortices adjacent to the bubbles show the streaming patterns observed. The black arrow indicates the direction of the bulk flow.

When cavities are placed adjacent to the channel, the microstreaming generated can either drive pumping or mixing [31, 32]. These cavities are known as lateral-cavity acoustic

transducers (LCAT). By changing the angle at which an array of cavities lie along the channel, the pumping efficiency can be altered [33]. The microstreaming seen in the LCAT array creates a third characteristic flow, known as the bulk flow. By varying the applied amplitude, Uo, Us and Ub all increase in magnitude. For this work, the LCAT and VCAT arrays provide on-chip pumping and mixing for the successful completion of an immunoassay.

2.5 Serodiagnostic Antigens

The diagnostic platforms, mentioned above, rely heavily on the detecting the presence of a single antigen. While this allows for simple and straightforward detection, this binary information doesn't provide information concerning a disease's progression. In order to monitor a disease's progression, multiple proteins need to be quantified. Protein microarrays and the field of proteomics and biomarker discovery can provide this type of analysis. Dr. Phil Felgner's protein microarray technology at UC Irvine has expanded microarrays to tests for a whole proteome of a given infectious agent. The development of this technology involves probing a large population to determine the key biomarkers for a given disease. These biomarkers would ideally provide information on whether a disease is present and the level of infection the disease that has manifested within the host. Following probing, the key biomarkers for the disease would be determined based on reactivity and variance in signal. Their lab has successfully developed a protein microarray for B. pseudomallei proteins with 10 biomarkers that can distinguish between positive and negative patient samples with 95% sensitivity and 83% specificity [34]. Diagnostics geared towards global health applications can greatly benefit from this simple detection platform and provide much needed information that is either too timely or costly to attain traditionally. However, because the microarrays are currently performed similarly to a macroscale immunoassay, it is not yet suitable for resource-limited settings. By using microfluidics, this technology could be amenable to these settings and be a key module in an integrated platform capable of providing a sample-to-answer analysis

Chapter 3
Research Design and Methods

3.1 Device Design

The two key characteristics of the immunoassay device were to implement both on-chip pumping and mixing with the use of the acoustic transducers and the nitrocellulose slides. There were several variations of nitrocellulose orientation on the slide, however due to high cost, slides containing 16 nitrocellulose pads were chosen to allow for multiple devices on one slide and further minimalize the amount of slides used. The dimensions of the nitrocellulose pads were 7.0mm x 7.0mm, so the following design of 3.2cm x 2.1cm was chosen to allow for two devices on one slide.

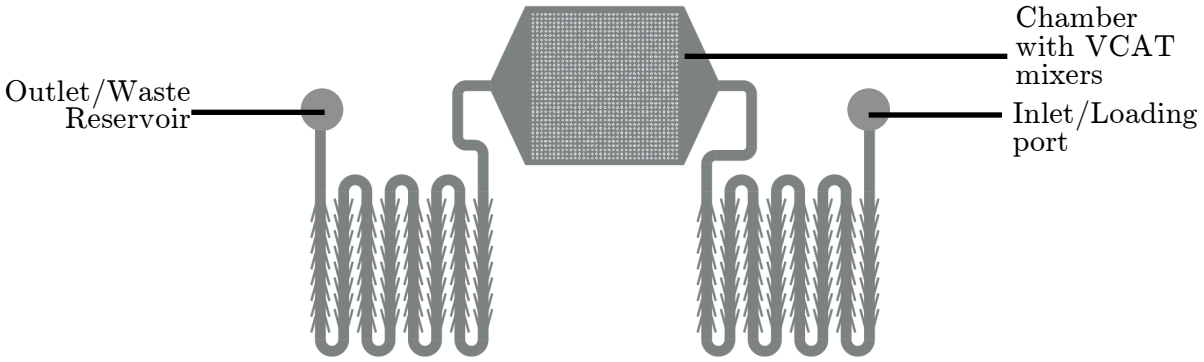

Figure 6. Microfluidic immunoassay platform using LCAT pumps and VCAT mixing

The chamber housing the nitrocellulose pad and the VCAT mixers is 7.2mm x 7.2mm and the LCAT side channels are 100um wide and 500um long, spaced 360um from each other. These side channels are positioned at a 15˚ angle to the main channel that is 500um wide, as this is the optimal pumping design shown in previous work [33]. The VCAT mixers are 100um in diameter spaced 100um apart, as this is the optimal mixing design shown in previous work [27].

3.2 Device Fabrication

To create the master mold, a 3" silicon wafer was first cleaned with 2% hydrofluoric acid to remove particles from the surface. Following dehydration, to fully dry the wafer, a layer of SU-8 2050 photoresist (MicroChem Corp.) was spin-coated onto the wafer at a height of 100 um. The wafer then underwent a soft-bake period, after which a transparency mask with the desired design was placed onto the wafer. The wafer was then exposed to UV lamp. Because SU-8 is a negative photoresist, the areas that are exposed to the UV light will become cross-linked and therefore, will not be soluble in developer. In the transparency mask, the design features are transparent, allowing for UV light to pass through onto the wafer, cross-link the SU-8 and create the mold for the devices. To complete the cross-linking process, the wafer underwent through a post-exposure bake period. For a single layer device, developer would be used to dissolve the unwanted SU-8 and go through a last hard-bake period to smoothen the features on the wafer. However, because the platform required a dual-layer device, a second-layer of SU-8 was spin-coated onto the wafer and the process wass repeated with a second transparency mask. Following the second post-exposure bake period, the developing and hard-bake processes were be carried out as for a single-layer device.

Upon completion of the master mold fabrication, a 1:5 of Teflon/FC-43 solution (3M) was spin-coated onto the wafer at 3000 rpm for 30 seconds and baked at 120 ˚C to functionalize the surface and prevent PDMS adhesion. Sylgard 184 elastomeric kit (Dow Corning Corp.) was used to make the PDMS polymer. A 10:1 ratio of polymer base to curing agent was mixed and poured onto the silicon wafer. The PDMS was cured at 60 ˚C for 24 hours and carefully peeled off the mold. Once the devices were cut, they were placed in a 120 ˚C oven for 24 hours to stiffen the PDMS. To create a complete device, the PDMS cast was contact-bonded to the glass slide with the nitrocellulose pads (Grace Biolabs) treated with Rain-X (SOPUS Products) to make the device as hydrophobic as possible.

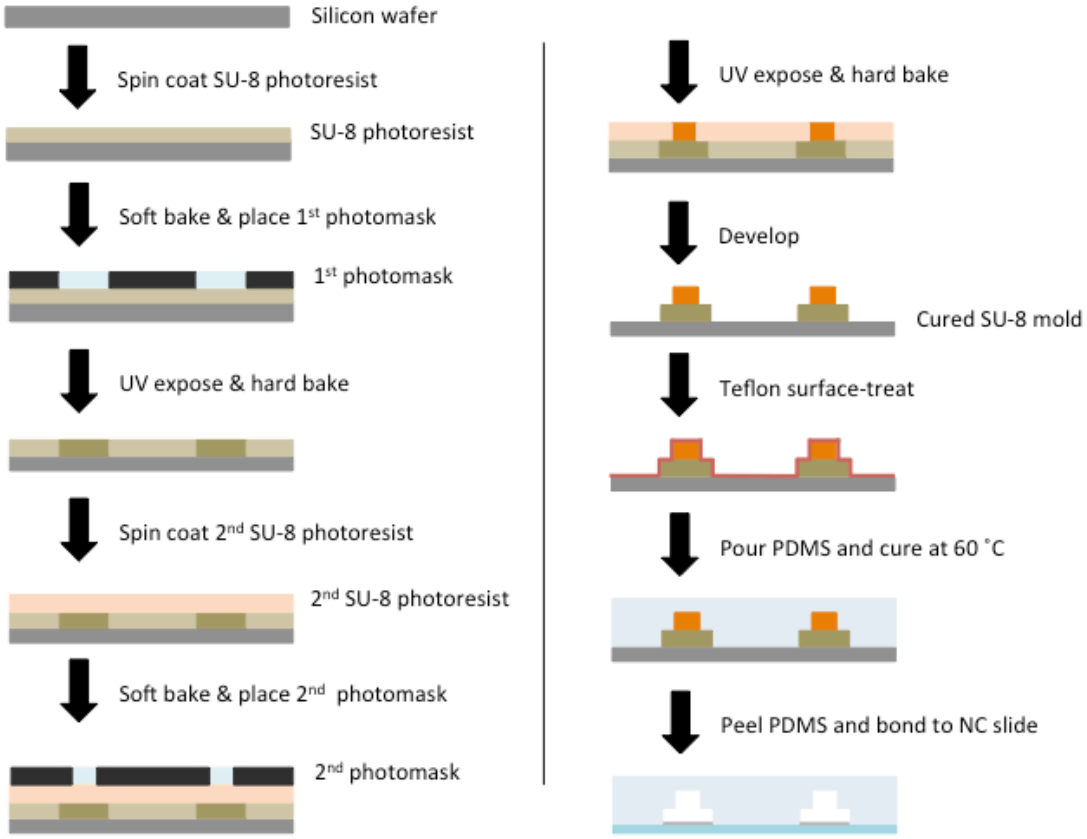

Figure 7. Illustration of dual-layer device fabrication with PDMS molding for complete device.

3.3 Experimental Setup

3.3.1 Device Operation

The device was first primed with protein blocking buffer (Maine Manufacturing) by introducing it into the outlet and pulling from the inlet using a syringe to fill the device and create the air-liquid interfaces needed for pumping and mixing. Once the buffer reached the inlet, 20 uL of the secondary antibody was placed into the inlet and the outlet was emptied of any excess fluid. The external acoustic energy source was supplied by a piezoelectric transducer (SMD43T105F200S, Steiner and Martins, Inc.). The devices were coupled to the PZT using AquaSonic Clear (Parker Labs Inc.) ultrasound gel. A square-wave signal of 50.55 kHz is applied to the PZT using a function generator (Agilent 33220A, Agilent Technologies) and voltage amplifier (Krohn-Hite 7500, Krohn-Hite Corp.) with a voltage of

8.25Vpp. Once the secondary antibody has been pumped through the device, the following reagents are introduced serially with a pipette.

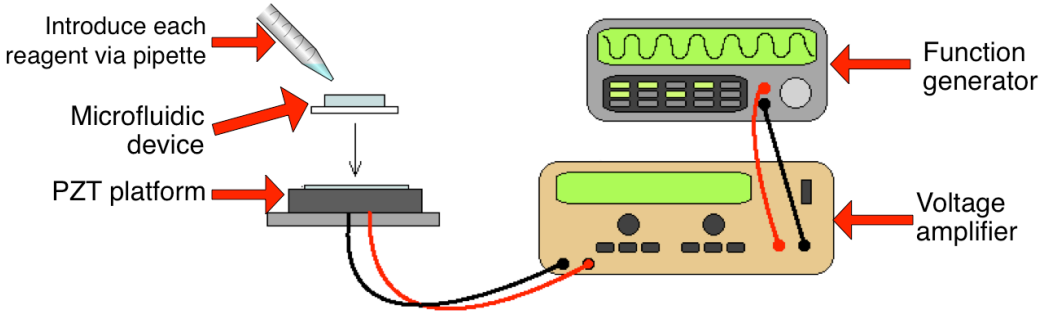

Figure 8. Diagram of Experimental Setup.

3.3.2 Serodiagnostic Antigens and Reagent Protocol

For characterization of the VCAT efficiency, a simple IgG-antibody assay was used. Human IgG was used because it is stable antibody that doesn't degrade in warm temperatures and it can be used as a diagnostic for diseases such as West Nile, Lyme disease, Dengue Virus and various other bacterial and fungal infections [20, 35-37]. By testing for a purified protein, the device could be sufficiently evaluated without the concerns of optimizing a protocol using serum and additional washing steps compromising with the results. The antigens (Catalog #009-000-003, Jackson ImmunoResearch Laboratories, Inc.) spotted were of varying concentration of human IgG antigen in the following format:

Table 1. Protein spot layout for characterization assays.

Top Left Corner	1	2	3	4	5
1	0 mg (PBS)	0.03 mg/mL	0.1 mg/mL	0.3 mg/mL	1 mg/mL
2	1 mg/mL	0.3 mg/mL	0.1 mg/mL	0.03 mg/mL	0 mg (PBS)
3	0 mg (PBS)	0.03 mg/mL	0.1 mg/mL	0.3 mg/mL	1 mg/mL
4	1 mg/mL	0.3 mg/mL	0.1 mg/mL	0.03 mg/mL	0 mg (PBS)
5	0 mg (PBS)	0.03 mg/mL	0.1 mg/mL	0.3 mg/mL	1 mg/mL

The table above illustrates how the antigens were spotted in both ascending and descending order; by spotting the antigens in this manner, the uniformity of flow through the chamber could be determined both qualitatively and quantitatively. The antigens are spotted using a 5x5 spotting pin array with an Omnigrid Accent Microarrayer (Genomic Solutions) that deposits 10nL of reagent onto the nitrocellulose pad. Each antigen spot has a diameter of roughly 440 um.

The IgG immunoassay consists of five reagents in order to evaluate the presence of IgG antibody in the sample: protein blocking buffer (Product #610485356, Maine Manufacturing), purified anti-human IgG antibody conjugated with alkaline phosphatase (AP) (Catalog #: 109-055-098, Jackson ImmunoResearch Laboratories, Inc.), Tris-tween buffered saline (TBST) as the wash solution (Sigma Aldrich), AP developing buffer (1-step NBT/BCIP) as the substrate solution (Catalog #34042, Thermo Fisher Scientific Inc.) and DI water as the stop solution. The purified anti-human IgG antibody solution is considered the sample for the characterization assays and is diluted 1:200 in blocking buffer. The spot intensity appears in relation to how much bound AP-conjugated secondary antibody cleaves the AP developing buffer and produces a dark purple hue .The figure below illustrates the binding process.

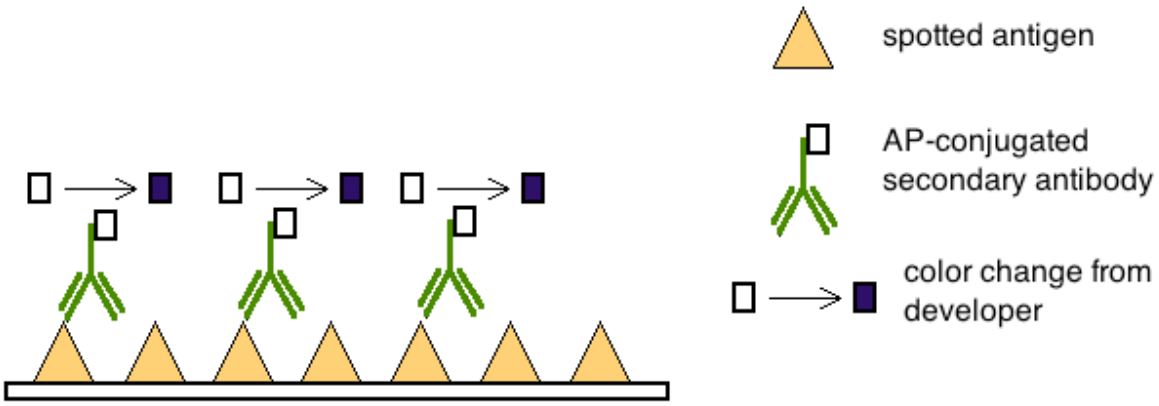

Figure 9. Illustration of IgG immunoassay for assay performance evaluation.

The test device is first filled with blocking buffer to create the air bubbles in the LCAT and VCAT arrays. Once it is coupled with the PZT, each reagent was introduced into the loading port and pumped through the device. The next reagent was loaded once the loading

port was emptied.

3.4 Spot Intensity Measurements

Upon completion of the immunoassay, results can be determined qualitatively. However, a quantitative approach is required to compare the sensitivity of each methodology. Therefore, an image was taken of each developed nitrocellulose pad, with the PDMS device removed from the slide. These photos were scanned using HP OfficeJet 4632 at 1200 dpi. In ImageJ, these photos were converted to a gray-scale, or 8-bit, image and processed to remove the background noise. Using a macro developed by Gilles Carpentier for ImageJ, the images were analyzed so that each spot was measured in relative fluorescent units (RFU) [38]. The above protocol was done for all microfluidic and traditional platforms and the results were compared statistically in GraphPad Prism v6.0c.

Chapter 4
Results

4.1 Assay Results

Because of the introduction of flow over the nitrocellulose pad and the continuous addition of reagents, it is expected that the assay will have improved sensitivity as well as reduce the operation time. Using a one-pump device and a simple IgG assay, the sensitivity of the simplified platform compared to a traditional assay procedure is determined. Each reagent is introduced into the loading port, only being refilled once the port has been completely drained. If the assay is successful, the spotted antigens become a dark purple hue as a result of the bound enzyme on the secondary antibody cleaving the developing buffer. The figure below is an example illustrates a successful assay where the spots indicate a binding reaction.

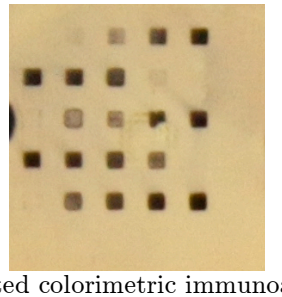

Figure 10. Completed colorimetric immunoassay on a nitrocellulose pad. Spots indicate bound antibody complexes; varying spot intensities indicate varying concentrations of spotted antibody.

The first experiment conducted was to determine whether the microfluidic platform could perform to the same standard as traditional methods. Normally, a simple IgG protein microarray takes 90 minutes using standard procedure. On average, each step mentioned in section 3.3.2.1 took about 5 minutes, totaling to 20 minutes for entire assay run time. First, the device was primed with blocking buffer to introduce air pockets in both the main channel and the chamber for the LCAT and VCAT arrays. The bubbles punched in the nitrocellulose pad chamber facilitate easy priming of the device and also allow air that may be trapped in the device to escape. Each reagent was introduced into the loading port and was refilled with the consequent reagent once the port had completely emptied. The table

below outlines the reagents in order of delivery, volumes and method of delivery for each reagent, necessary for assay completion.

Table 2. Protocol for reagent delivery in microfluidic devices.

Reagent	Volume	Method of Delivery
Blocking Buffer	25uL	Flowed using negative pressure with a syringe
Secondary antibody solution	20uL	Pumped and mixed
TBST wash solution	20uL	Pumped and mixed
1 step NBT/BCIP developer	20uL	Pumped and mixed
DI water stop solution	20uL	Pumped and mixed

Comparison of spot intensities between both microfluidic and traditional assay platforms are shown in the following figure. Blue bars represent results from the traditional assay and red bars represent results from the microfluidic platform. Error bars are SD.

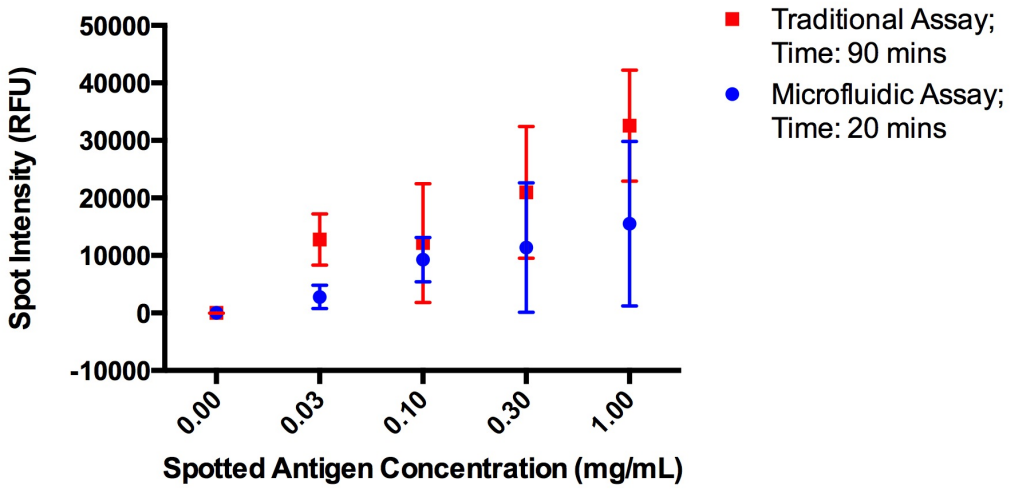

Figure 11. Comparison of spot intensities between both microfluidic and traditional assay platforms. Blue dots represent results from the microfluidic assay and red bars represent results from the traditional platform. Error bars are SD for n=5.

As seen in the figure above, there is a signal for all the spots using the microfluidic device, however it is not comparable to the results that one would get using a traditional assay platform, despite using the same secondary antibody dilution of 1:200. However, it is hopeful that this signal can be improved by optimizing the dilution of the secondary antibody to get results similar to the control of the traditional assay. This would be

advantageous as one would observe the same intensities as seen with a traditional platform but the run time is significantly decreased.

To determine which dilution of secondary antibody is optimal for the microfluidic assay, the experiments were conducted using the same protocol outlined in Table 2 but with varying dilutions of secondary antibody. These dilutions varied from 1:200 to 1:1600 and were compared with the control of a developed nitrocellulose pad from a standard microarray platform. Comparisons of the different dilutions can be seen in Figure 12.

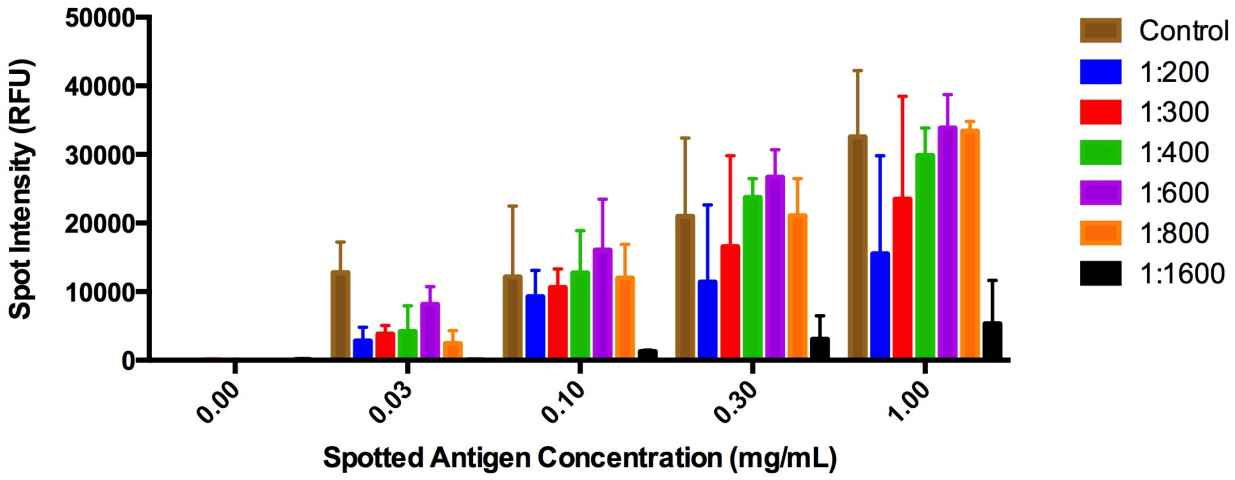

Figure 12. Comparisons of varying dilutions of secondary antibody. Brown bars represent results from a standard microarray platform conducted in 90 minutes. Blue bars represent a 1:200 dilution, red bars represent a 1:300 dilution, green bars represent a 1:400 dilution, purple bars represent a 1:600 dilution, orange bars represent a 1:800 dilution and black bars represent a 1:1600 dilution. Error bars are SD with n=5.

As seen above, there is an increased signal for dilutions higher than 1:200 for each of the spotted antibodies on the nitrocellulose pad. At 0.10 and 0.30 mg/mL, there is a more pronounced bell curve in intensity, resulting from the competitive binding between the antibody and the precipitate. This is characteristic of most precipitation reactions, where the peak of the curve that plateaus in signal before decreasing again is known as the equivalence zone [39]. From the plots, the equivalence zone is between the dilutions of 1:400 and 1:600. For the following experiments, a working dilution of 1:400 was used for the secondary antibody.

To verify that the introduction of flow and convective mixing were responsible for the acquired signal and if so, what was the difference in signal, another experiment was

conducted where an assay was completed within the microfluidic device with and without the actuated pumping and mixing. The protocol and results of these experiments are found below, where every step was unvaried (including incubation/pumping time) except for the method of delivery:

Table 3. Protocol for actuated pumping and mixing vs. passive microfluidic devices

Reagent	Volume	Method of Delivery
Blocking Buffer	25uL	Flowed using negative pressure with a syringe
1:400 dilution of secondary antibody	20uL	Flowed using negative pressure with a syringe OR pumped and mixed
TBST wash solution	20uL	Flowed using negative pressure with a syringe OR pumped and mixed
1-step NBT/BCIP Developer	20uL	Flowed using negative pressure with a syringe OR pumped and mixed
DI water stop solution	20uL	Flowed using negative pressure with a syringe OR pumped and mixed

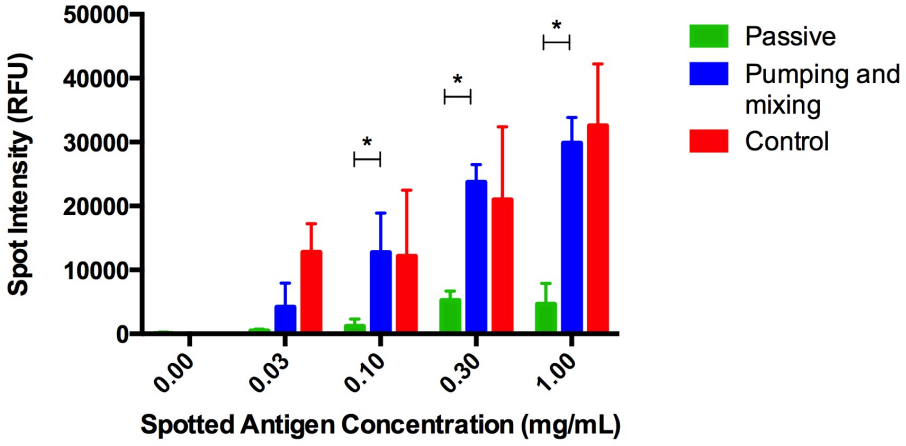

Figure 13. Spot intensities of passive and actuated microfluidic devices in comparison with standard control. The green bars represent results from the passive microfluidic device, the blue bars represent results from actuated pumping and mixing and the red bars represent results from the standard microarray. Error bars are SD for n=5 and asterisks signifiy statistical significance between passive and pumping and mixing bars ($P < 0.05$).

As seen in Figure 13, results from the passive microfluidic device are significantly lower compared to the actuated device, especially at the higher spotted concentrations. At these lower spot intensities, it could be hard to distinguish what is a significant signal when using a passive device and would not be a reliable method in determining the presence of an antibody.

Because the microfluidic platform has higher flow velocities, it is possible that the increased signal could be because of higher binding efficiency introduced to fluid being flowed instead of being static. Previous work has shown that flow-through assays exhibit higher signals compared to passive assays, as well [40]. To determine whether or not the VCATs contributed to the higher signal, the characterization device was fabricated without the VCATs so that it would act as a flow through assay. Using the flow through device, the same steps were performed as mentioned in section 3.3.2.1. The results are illustrated in the figure below.

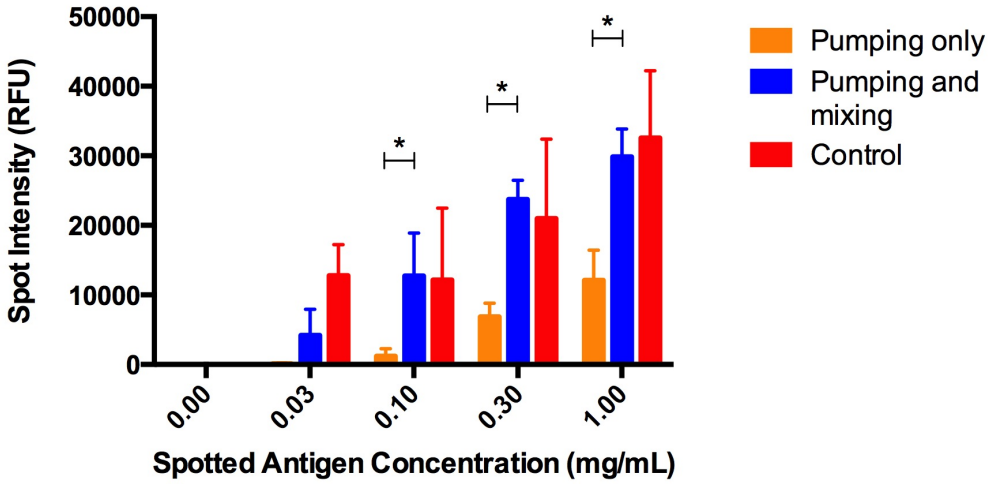

Figure 14. Spot intensities of only actuated pumping or actuated pumping and mixing microfluidic devices compared to standard microarray platform. Orange bars represent only actuated pumping results, blue bars represent actuated pumping and mixing results and red bars represent standard microarray results. Error bars are SD for n=5 and asterisks signify statistical significance between only actuated pumping and actuated pumping and mixing bars ($P < 0.05$).

Figure 14 shows that while there is an increase in signal with only actuated pumping when compared to the passive device, it does not provide the intensities that are observed with both actuated pumping and mixing. Additionally, there is at least a two-fold difference

between the flow-through and actuated pumping and mixing devices, with the higher spotted concentrations demonstrating statistical significance in their difference. This leads to the conclusion that acoustic cavity-induced convective mixing and pumping in this platform are essential for comparable signal intensities with minimal run time.

Chapter 5
Discussion

5.1 Optimization Work

There are two main areas in where this platform can be further expanded, one of which is optimizing the platform. In comparison to the traditional microarray platform, the microfluidic LCAT/VCAT device is able to perform to same standard but with less reagent volumes and run times. However, there are areas where this platform needs to be improved. For instance, because the entire device is actuated by one PZT, pumping and mixing are not separated in this platform and therefore, the assay performance is dependent on the applied voltage. Previously conducted experiments have shown that devices tested at lower than 8.25Vpp greatly increase the run time with similar results to those tested at 8.25Vpp. However, testing devices that increase run time can undermine the device towards the end of completion as the bubbles driving pumping in the LCAT arrays expand and consequently, make pumping in the device less efficient. The figure below illustrates this phenomenon.

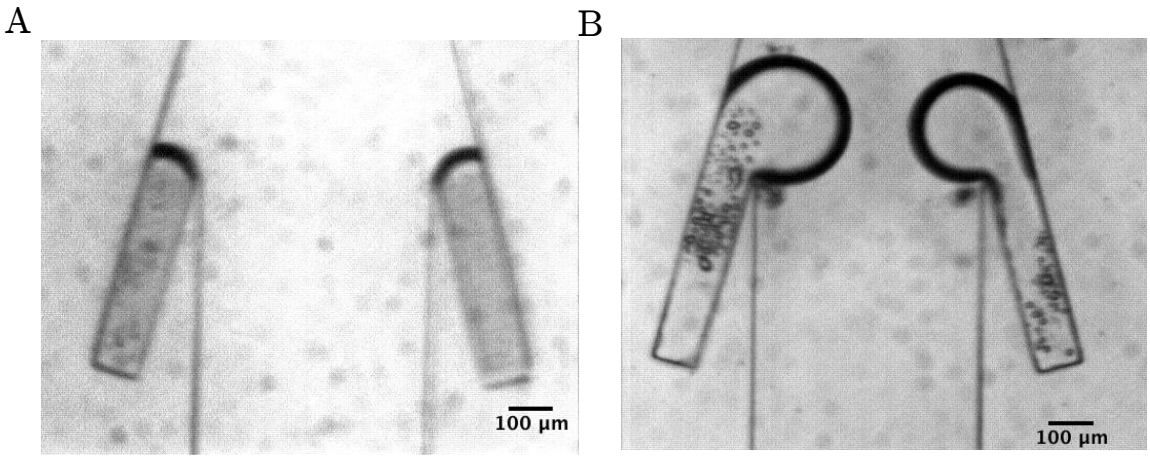

Figure 15. Normal and expanded LCAT pairs. (A) An LCAT pair at t=0mins (at the beginning to the test) (B) An LCAT pair at t=20mins (at the end of the test)

Conversely, devices tested at voltages higher than 8.25Vpp achieve very fast run times, however, the reagents are passed through the device so quickly that convective mixing is not able to take place. Therefore, results similar to the Figure 14 are observed with

diminished spot intensities. Therefore, using this setup requires a balance of pumping at reasonable rate while still allowing mixing to occur. If these two processes were separated, then experiments could be conducted on what applied voltages provide optimal mixing. This would also allow pumping and mixing to be independent of each other as after the fluid is pumped in the VCAT mixing chamber, the LCAT pumps could be turned off and no longer affect the fluid manipulation in the chamber.

Another area of optimization involves the slides with the adhered nitrocellulose pads. Because the pads are traditional thick microscope slides, they require more acoustic energy to be able to dissipate through the slide and actuate the air-liquid interfaces. By adhering the nitrocellulose onto a thinner substrate, a lower voltage could be applied and not only lower the amount of power consumed but also minimize some of the expanding behavior mentioned above.

5.2 Future Work

The end goal for this platform is for it to be a fully automated platform for point-of-care applications. Therefore there are two major areas of future work. The first is to expand this device so that it will be able to perform an immunoassay with a sample of human serum. The use of human serum will also require re-optimizing the platform, as serum requires sample preparation and purification steps. Because human serum is also abundant in other antibodies and proteins that can cause non-specific binding within the assay, additional wash steps may have to be included. To better accomplish this, the device needs to be expanded so that each reagent has its own pump and to create a platform where each LCAT and VCAT arrays are actuated by a separate PZT. This will minimize the issues that were observed and mentioned above (bubble expansions and codependence of pumping and mixing) and also facilitate ease of use. The second area of future work involves creating an electronics portion that will control the actuation of these PZTs and can be operated with low power consumption. Our current setup is bulky and requires a stable electricity source. By miniaturizing the platform so that it is portable, power consumption is less of a

concern and can provide healthcare information to a variety of settings. An envisioned platform of this nature is rendered in the figure below.

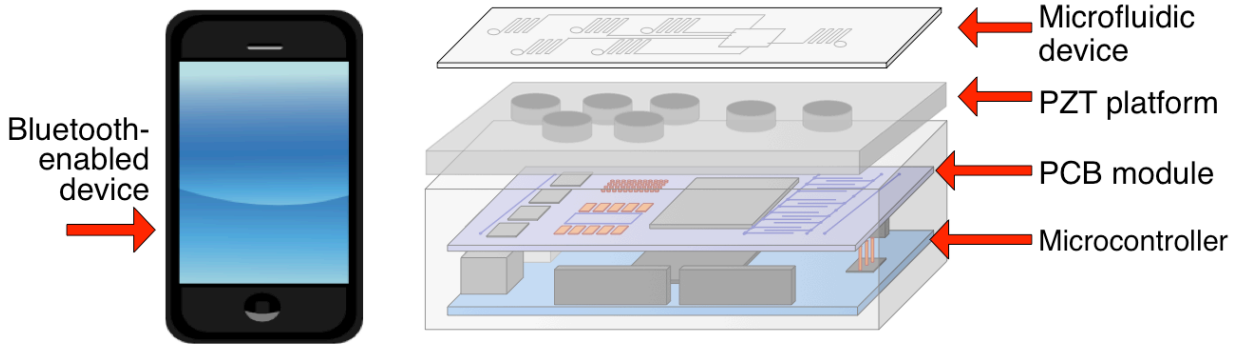

Figure 16. A portable immunoassay platform for point-of-care applications

The system above would be 6" x 4" x 4" ideally, to minimize its footprint, and the microfluidic device would have the same dimensions as a standard microfluidic slide, with design features embossed in plastic and adhered to the slide. The device would sit on a PZT platform connected to the PCB module and microcontroller. These two latter components would contain and control the individual electronics for individual PZT actuation. The PZT platform can be modified depending on the range of flow rates required for the immunoassay. If using air transducers (weaker PZTs), higher voltages are required to drive pumping and would therefore require an established electrical source, such as a D.C. power supply. However if small solid disc-PZTs are used, lower voltages are required and could be powered by two rechargeable 9V batteries in series. By using a Bluetooth-enabled device, the individual PZTs can be actuated by activating a signal with a given frequency and voltage using a phone application. Ideally, the phone application would allow for alterations in voltage to better manipulate flow and mixing rates so that the platform could be amenable to different immunoassays. This setup only allows for qualitative readings of the results, however, another application could be developed to allow for measuring spot intensity and determining diagnoses from these results using a picture taken with the camera phone. A platform of these specifications would provide essential health care information for point-of-care applications and could better evaluate a patient's health status for a given disease progression.

Chapter 6
References

[1] A. Boutayeb, "The Burden of Communicable and Non-Communicable Diseases in Developing Countries," in *Handbook of Disease Burdens and Quality of Life Measures*, V. Preedy and R. Watson, Eds., ed: Springer New York, 2010, pp. 531-546.

[2] D. Mabey, R. W. Peeling, A. Ustianowski, and M. D. Perkins, "Tropical infectious diseases: Diagnostics for the developing world," *Nat Rev Micro,* vol. 2, pp. 231-240, 03//print 2004.

[3] P. Yager, T. Edwards, E. Fu, K. Helton, K. Nelson, M. R. Tam*, et al.*, "Microfluidic diagnostic technologies for global public health," *Nature,* vol. 442, pp. 412-418, 07/27/print 2006.

[4] C. A. Heid, J. Stevens, K. J. Livak, and P. M. Williams, "Real time quantitative PCR," *Genome research,* vol. 6, pp. 986-994, 1996.

[5] E. Eteshola and D. Leckband, "Development and characterization of an ELISA assay in PDMS microfluidic channels," *Sensors and Actuators B: Chemical,* vol. 72, pp. 129-133, 2001.

[6] H. Kaur, J. Dhanao, and A. Oberoi, "Evaluation of rapid kits for detection of HIV, HBsAg and HCV infections," *Indian journal of medical sciences,* vol. 54, p. 432, 2000.

[7] A. A. Raj, T. Subramaniam, S. Raghuraman, and P. Abraham, "Evaluation of an indigenously manufactured rapid immunochromatographic test for detection of HBsAg," *Indian J Pathol Microbiol,* vol. 44, pp. 413-4, Oct 2001.

[8] G. Zhang, J. Guo, and X. Wang, "Immunochromatographic lateral flow strip tests," in *Biosensors and biodetection*, ed: Springer, 2009, pp. 169-183.

[9] P. Von Lode, "Point-of-care immunotesting: approaching the analytical performance of central laboratory methods," *Clinical biochemistry,* vol. 38, pp. 591-606, 2005.

[10] G. A. Posthuma-Trumpie, J. Korf, and A. van Amerongen, "Lateral flow (immuno) assay: its strengths, weaknesses, opportunities and threats. A literature survey," *Analytical and bioanalytical chemistry,* vol. 393, pp. 569-582, 2009.

[11] G. Hu, Y. Gao, and D. Li, "Modeling micropatterned antigen–antibody binding kinetics in a microfluidic chip," *Biosensors and Bioelectronics,* vol. 22, pp. 1403-1409, 2/15/ 2007.

[12] D. Mark, S. Haeberle, G. Roth, F. von Stetten, and R. Zengerle, "Microfluidic lab-on-a-chip platforms: requirements, characteristics and applications," *Chemical Society Reviews,* vol. 39, pp. 1153-1182, 2010.

[13] D. R. Gossett, W. M. Weaver, A. J. Mach, S. C. Hur, H. T. K. Tse, W. Lee*, et al.*, "Label-free cell separation and sorting in microfluidic systems," *Analytical and bioanalytical chemistry,* vol. 397, pp. 3249-3267, 2010.

[14] A. A. S. Bhagat, H. Bow, H. W. Hou, S. J. Tan, J. Han, and C. T. Lim, "Microfluidics for cell separation," *Medical & biological engineering & computing,* vol. 48, pp. 999-1014, 2010.

[15] C. H. Chen, S. H. Cho, F. Tsai, A. Erten, and Y.-H. Lo, "Microfluidic cell sorter with integrated piezoelectric actuator," *Biomedical microdevices,* vol. 11, pp. 1223-1231, 2009.

[16] J. S. Marcus, W. F. Anderson, and S. R. Quake, "Microfluidic single-cell mRNA isolation and analysis," *Analytical chemistry,* vol. 78, pp. 3084-3089, 2006.

[17] R. H. Liu, J. Yang, R. Lenigk, J. Bonanno, and P. Grodzinski, "Self-contained, fully integrated biochip for sample preparation, polymerase chain reaction amplification, and DNA microarray detection," *Analytical chemistry,* vol. 76, pp. 1824-1831, 2004.

[18] S. K. Sia, V. Linder, B. A. Parviz, A. Siegel, and G. M. Whitesides, "An Integrated Approach to a Portable and Low - Cost Immunoassay for Resource - Poor Settings," *Angewandte Chemie International Edition,* vol. 43, pp. 498-502, 2004.

[19] T. M. Daniel, "Rapid Diagnosis of Tuberculosis: Laboratory Techniques Applicable in Developing Countries," *Review of Infectious Diseases,* vol. 11, pp. S471-S478, March 1, 1989 1989.

[20] G. Tardei, S. Ruta, V. Chitu, C. Rossi, T. Tsai, and C. Cernescu, "Evaluation of immunoglobulin M (IgM) and IgG enzyme immunoassays in serologic diagnosis of West Nile virus infection," *Journal of clinical microbiology,* vol. 38, pp. 2232-2239, 2000.

[21] C. D. Chin, Y. K. Cheung, T. Laksanasopin, M. M. Modena, S. Y. Chin, A. A. Sridhara*, et al.*, "Mobile device for disease diagnosis and data tracking in resource-limited settings," *Clinical chemistry,* vol. 59, pp. 629-640, 2013.

[22] K. Kriz, F. Ibraimi, M. Lu, L.-O. Hansson, and D. Kriz, "Detection of C-reactive protein utilizing magnetic permeability detection based immunoassays," *Analytical chemistry,* vol. 77, pp. 5920-5924, 2005.

[23] A. Bhattacharyya and C. M. Klapperich, "Design and testing of a disposable microfluidic chemiluminescent immunoassay for disease biomarkers in human serum samples," *Biomed Microdevices,* vol. 9, pp. 245-51, Apr 2007.

[24] S. Elder and W. L. Nyborg, "Acousting streaming resulting from a resonant bubble," *The Journal of the Acoustical Society of America,* vol. 28, p. 155, 1956.

[25] W. L. Nyborg, "Acoustic streaming near a boundary," *The Journal of the Acoustical Society of America,* vol. 30, pp. 329-339, 1958.

[26] P. Marmottant and S. Hilgenfeldt, "Controlled vesicle deformation and lysis by single oscillating bubbles," *Nature,* vol. 423, pp. 153-6, May 8 2003.

[27] Y. Okabe, Y. Chen, R. Purohit, R. M. Corn, and A. P. Lee, "Piezoelectrically driven vertical cavity acoustic transducers for the convective transport and rapid detection of DNA and protein binding to DNA microarrays with SPR imaging—A parametric study," *Biosensors and Bioelectronics,* vol. 35, pp. 37-43, 5/15/ 2012.

[28] P. Marmottant and S. Hilgenfeldt, "A bubble-driven microfluidic transport element for bioengineering," *Proc Natl Acad Sci U S A,* vol. 101, pp. 9523-7, Jun 29 2004.

[29] R. H. Liu, R. Lenigk, R. L. Druyor-Sanchez, J. Yang, and P. Grodzinski, "Hybridization enhancement using cavitation microstreaming," *Anal Chem,* vol. 75, pp. 1911-7, Apr 15 2003.

[30] M. V. Patel, A. R. Tovar, and A. P. Lee, "Lateral cavity acoustic transducer as an on-chip cell/particle microfluidic switch," *Lab Chip,* vol. 12, pp. 139-45, Jan 7 2012.

[31] A. R. Tovar and A. P. Lee, "Lateral cavity acoustic transducer," *Lab on a Chip,* vol. 9, pp. 41-43, 2009.

[32] A. Doria, N. E. Martin, and A. P. Lee, "Rapid Quantification OF C-Reactive Protein Agglutination with Acoustic-Enabled Microvortices," presented at the 16th International

Conference on Miniaturized Systems for Chemistry and Life Sciences (uTAS), Oct. 28 - Nov. 1, 2012, Okinawa, Japan.

[33] A. R. Tovar, M. V. Patel, and A. P. Lee, "Lateral air cavities for microfluidic pumping with the use of acoustic energy," *Microfluidics and Nanofluidics,* vol. 10, pp. 1269-1278, 2011.

[34] P. L. Felgner, M. A. Kayala, A. Vigil, C. Burk, R. Nakajima-Sasaki, J. Pablo*, et al.*, "A *Burkholderia pseudomallei* protein microarray reveals serodiagnostic and cross-reactive antigens," *Proc Natl Acad Sci U S A,* vol. 106, pp. 13499-13504, August 11, 2009 2009.

[35] V. P. Berardi, K. E. Weeks, and A. C. Steere, "Serodiagnosis of Early Lyme Disease: Analysis of IgM and IgG Antibody Responses by Using an Antibody-Capture Enzyme Immunoassay," *The Journal of Infectious Diseases,* vol. 158, pp. 754-760, 1988.

[36] J. Groen, P. Koraka, J. Velzing, C. Copra, and A. D. M. E. Osterhaus, "Evaluation of Six Immunoassay for Detection fo Dengue Virus-Specific Immunoglobulin M and G Antibodies," *Journal of clinical microbiology,* vol. 7, pp. 867-871, 2000.

[37] J. Petitjean, A. Vabret, S. Gouarin, and F. Freymuth, "Evaluation of Four Commercial Immunoglobulin G (IgG)- and IgM-Specific Enzyme Immunoassays for Diagnosis of *Mycoplasma pneumoniae* Infections," *Journal of clinical microbiology,* vol. 40, pp. 165-171, 2002.

[38] G. Carpentier and E. Henault, "Protein Array Analyzer for ImageJ," presented at the Proceedings of the ImageJ User and Developer Conference, 2010.

[39] H. H. Sussman, J. Parker A. Small, and E. Cotlove, "Human Alkaline Phosphatase Immunochemical Identification of Organ-Specific Isoenzymes," *The Journal of Biological Chemistry,* vol. 243, pp. 160-166, 1968.

[40] L. Yu, C. M. Li, Y. Liu, J. Gao, W. Wang, and Y. Gan, "Flow-through functionalized PDMS microfluidic channels with dextran derivative for ELISAs," *Lab on a Chip,* vol. 9, pp. 1243-1247, 2009.